

Electroosmotic flow in polymer-coated slits: a joint experimental/simulation study

Michele Monteferrante · Simone Melchionna ·
Umberto Marini Bettolo Marconi · Marina Cretich ·
Marcella Chiari · Laura Sola

Received: 20 December 2013 / Accepted: 9 June 2014
© Springer-Verlag Berlin Heidelberg 2014

Abstract The quality of separation in capillaries electrophoresis is strongly affected by the magnitude of the electroosmotic flow (EOF). The EOF can be efficiently suppressed by coating the capillary wall with hydrophilic polymers. In this paper, experimental data are presented to show the effect of coating thickness and charge on mass transport. Simulations performed with the lattice Boltzmann technique quantitatively reproduce the EOF with and without the coating and with either a neutral or charged coating layer. Experimental, simulation and theoretical analyses converge toward the interpretation that EO suppression arises from the frictional forces acting on the ionic currents and that a detailed representation of the polymeric coating is not needed in order to capture the phenomenon.

1 Introduction

One of the most important features of capillary and microchip electrophoresis is the electroosmotic (EO) flow (Bruus

2008; Masliyah and Bhattacharjee 2006). This electrokinetic phenomenon originates from the presence onto the capillary surface of negative charges that form when the microchannel is placed in contact with any aqueous solution. This layer of immobilized charges causes adsorption of positive counter-ions from the buffer solution with formation of an electric double layer, the so-called Debye layer. The application of an electric field parallel to the surface causes the diffuse ions of the double layer and their surrounding water molecules to migrate toward the cathode generating a flow of liquid in the capillary. This flow has dramatic influences on the time the analytes reside inside the capillary. The importance of controlling electroosmotic flow (EOF) has been long recognized in the community working on micro- and nano-fluidics of electrolytic solutions. Many groups, including our own, have experimentally demonstrated that the EO mobility in channels of micrometer size is suppressed by more than one order of magnitude when the channel walls are coated with neutral polymers anchored onto the wall surface (Chiari et al. 2000; Horvath and Dolník 2001; Znaleziona et al. 1999). It is generally accepted that, in order to reduce substantially the EOF, the thickness of the polymer film must be larger than the Debye length. Experimental data indicated that the chemical nature of the coating polymer strongly impacts the EOF suppression capabilities and that a critical polymer chain length is required in order to quench effectively the EOF (Doherty et al. 2002).

In this paper, we investigate the influence of the thickness of adsorbed polymer coatings on EOF in capillary electrophoresis using numerical simulations. Our results provide useful guidelines for the design of new coatings. In previous studies, the suppression of EO flow has been investigated via molecular dynamics simulation approach (Tessier and Slater 2005; Grass et al. 2009; Tessier and Slater 2006). One of the main objectives of previous

M. Monteferrante · M. Cretich · M. Chiari · L. Sola
Consiglio Nazionale delle Ricerche, Istituto di Chimica del
Riconoscimento Molecolare (ICRM-CNR), Via Mario Bianco,
20131 Milan, Italy

S. Melchionna (✉)
Dipartimento di Fisica, Consiglio Nazionale delle Ricerche,
Istituto dei Processi Chimico-Fisici (IPCF-CNR),
Università La Sapienza, P.le A. Moro2, 00185 Rome, Italy
e-mail: simone.melchionna@gmail.com

U. M. B. Marconi
Scuola di Scienze e Tecnologie, Università di Camerino
and Istituto Nazionale di Fisica Nucleare (PG),
Via Madonna delle Carceri, 62032 Camerino, Italy

computational studies was to compare simulation data with the theoretical predictions put forward by Harden et al. (2001). In the limit of an infinitely thin Debye layer, the theory predicts that at low coverage, in the so-called mushroom regime, the EO mobility decreases linearly with the coverage parameter. At sufficiently high coverage, in the so-called brush regime, the EO mobility scales in a highly nontrivial way with the degree of coverage. Slater et al. (2009) performed extensive simulations on a coated cylindrical channel with finite Debye layer thickness. They found a significant EOF reduction and good agreement between theoretical and experimental EOF values (Hickey et al. 2009, 2011). In particular, they observed a complete EOF suppression at a coverage density well below the brush regime, together with the occurrence of flow reversal for charged polymer coatings (Horvath and Dolník 2001). A direct quantitative comparison with experiments is typically difficult due to the limited size of the simulated system and the use of large salinity, an inherent limitation of the employed computational approach. Other authors studied the effect of polymer structure and solvent characteristics on EOF, as well as its dependence on the applied electric field (Quiao and He 2007; Cao et al. 2010). Mesoscopic modeling and simulations were employed to study how the strength of polymer absorption affects the EOF, showing that the more strongly a chain is absorbed on a surface, the less it quenches the EOF (Hickey et al. 2009), in good agreement with the experimental findings of Doherty et al. (2002).

Notwithstanding the successful convergence of experiments, theory and simulations, a complete understanding of the mechanisms governing EOF suppression is still missing. In particular, it is highly desirable to identify the minimal conditions that efficiently suppress electroosmosis. Even if a particle-based simulation method such as molecular dynamics can provide a detailed microscopic understanding of how EOF suppression takes place, a more mesoscopic approach enables us to investigate the phenomenon by taking into account only a minimal set of physical requirements. To this purpose, we adopt here a strategy that employs the lattice Boltzmann (LB) mesoscopic techniques (Benzi et al. 1992; Melchionna and Marconi 2011, 2012) to simulate an electrolytic solution flowing in a charged slit channel. In addition, we model the polymer coating in effective terms as a scattering medium that describes the frictional forces exerted between the solvent and ionic species with the polymer layer.

In the current experimental setup, the thickness of the coating is much smaller than the channel radius and about five times larger than the Debye layer. Previous results demonstrated that it is sufficient to reach such coating thickness to suppress effectively the EO flow (Sola and Chiari 2012). The importance of controlling surface properties resides in the fact that EO fluid transport disturbs measurements performed with such devices whereas finely controlled EO conditions can strongly improve the performance of electrophoretic separations.

2 Methods

2.1 Experimental method

The experimental micro-channel is composed of a SiO₂ glass. As well documented in the literature, by changing the pH of the solution, the surface charge density of the material is modified by the dissociation equilibrium. The EO flow was therefore experimentally measured at different pH values in coated and uncoated capillaries using the following running buffers (all at a constant ionic strength of 18 mM): H₃PO₄–NaOH pH 2.5, 6-ε-aminocaproic acid–acetic acid pH 4.4, H₃PO₄–NaOH pH 7.0 and Bicine-TRIS pH 8.5. An extensive description of the polymer coating used is reported in Sola and Chiari (2012).

Thickness and density of the polymer coating were determined using Analight Bio 200 an instrument based on dual polarization interferometry, a label-free technique, that measures the layer thickness of thin films on surfaces with picometer resolution. Table 1 shows mass, thickness and density of the polymer films analyzed in this study and previously reported in reference (Sola and Chiari 2012).

The fused silica capillaries utilized in this study had the following dimensions: 50 μm ID, 54 cm total length and 44 cm to detection window. The capillaries were filled with buffer, and the EO flow was measured and calculated using the pressure mobilization method as described in Williams and Vigh (1996). A 0.8 % w/v aqueous solution of acrylamide, dissolved in each buffer, was used as neutral marker.

2.2 Theoretical method

In order to give a self-contained presentation, we recall that for an uncoated slit channel, the Helmholtz–Smoluchowski

Table 1 Thickness, mass and density of polymer coatings

Surface coating	Thickness (nm)	Mass (ng/mm ²)	Density (g/cm ³)
Poly(DMA–GMA–MAPS)	9.2 ± 0.9	1.6 ± 0.02	0.179 ± 0.015
Poly(DMA–NAS–MAPS)	13.6 ± 3.8	1.4 ± 0.01	0.105 ± 0.03

equation relates the EO flow velocity as a function of the applied electric field and other quantities stemming from the electrolytic solution, and reads:

$$v_x(y) = -\frac{\epsilon E_x \zeta}{\eta} \left[1 - \frac{\cosh(k_D y)}{\cosh(k_D w)} \right], \quad (1)$$

where $v_x(y)$ is the velocity profile along the flow direction x , E_x is the applied electric field, and the transverse direction is oriented along the y axis. In Eq. (1), k_D is the inverse Debye length, ϵ is the dielectric susceptibility, ζ is the zeta potential, η is the dynamic viscosity of the solution, and $2w$ is the separation between the planes. Equation (1) is valid in the low potential regime, which allows for the linearization of the Poisson–Boltzmann equation, whose validity can be verified a posteriori by simulations. Moreover, when $k_D w \gg 1$ (thin layer approximation), the term in parenthesis can be taken as unity, and the simpler relation holds:

$$v_x = -\frac{\epsilon E_x \zeta}{\eta}. \quad (2)$$

As apparent, the velocity does not depend on y and it is equal to the flow velocity at the channel center, which also corresponds to the maximum value of $v_x(y)$. Using the above relation, the EO mobility is defined as the ratio between the velocity and the electric field:

$$\mu = \epsilon \frac{\zeta}{\eta}. \quad (3)$$

For a flat wall, the surface charge density Σ satisfies the Grahame equation:

$$\Sigma(\zeta) = \frac{2\epsilon k_D}{\beta e} \sinh \left[\frac{\beta e \zeta}{2} \right], \quad (4)$$

where e is the electron charge and $\beta = 1/k_B T$ the inverse thermal energy. Equation (4) is derived using the Gouy–Chapman theory and assuming the electro-neutrality condition. Equations (3, 4) are used in this work in order to infer the correspondence between the pH value and the surface charge density of silica which must be given as input parameter in our simulations. Even if, in principle, the surface charge density of silica at varying pHs could be theoretically estimated by a dissociation model (Grier and Behrens 2001), such an approach fails to consider the presence of a buffer which is employed in actual experiments.

However, since we are only interested in explaining the effect on the EO mobility of the polymer coating, we took the experimental result in the absence of coating to determine the surface charge density as follows: Given the experimentally measured values of the EO mobility, μ_{ex} , the zeta potential is obtained from Eq. (3) and the surface charge density from Eq. (4):

$$\Sigma(\zeta) = \frac{2\epsilon k_D}{\beta e} \sinh \left[\frac{\beta e \mu_{ex} \eta}{2\epsilon} \right]. \quad (5)$$

The surface charge density obtained for a given value of the pH is used in the simulation. In Figs. 2, 3 and 4, in order to obtain a more direct comparison with experiments, we report the mobilities as a function of pH instead of the surface charge density.

2.3 Computational method

Our computational approach is based on a kinetic description of a ternary mixture composed of a neutral solvent and two monovalent electrolytes. The dynamics of the charged system can be casted as a numerical method in the framework of the so-called LB method (Melchionna and Marconi 2011, 2012). An overview of the approach is reported in the “Appendix”.

In order to reproduce the experimental setup, we considered the same Debye length of the experiments, $k_D^{-1} = 2.3$ nm, corresponding to an ionic strength of 18 mM. The Bjerrum length, the kinematic viscosity and the density correspond to the values of water at room temperature equal to 0.7 nm, 10^{-6} m²/s and 1 g/cm³, respectively. The concentration of the charge carriers is obtained by imposing the condition of global electro-neutrality for a given surface charge density and with the fixed value of the Debye length.

At variance with experiments, where the EO flow is measured in a cylindrical capillary, for the simulations and the theoretical model, we considered the case of slit channels, whereas the difference of the calculated quantities with respect to the cylindrical channel is expected to be of the order of 5 % or below (Grier and Behrens 2001). For the simulation setup, we constructed a three-dimensional mesh composed of $40 \times 250 \times 10$ grid points, with a mesh spacing of 0.1 nm, which resolves accurately the double layer. The LB unit charge is equal to the elementary electron charge, and the timestep is $\delta t = 10$ fs. The external electric field is homogeneous and applied along the x direction, and the electroosmotic mobility is calculated as v_M/E_x with v_M being the fluid velocity at the channel center. Using v_M to calculate the mobility is appropriate to compare the results with experimental findings with respect to averaging the velocity along the transverse section. In fact, experiments are usually performed at $k_D w \gg 1$ and in this limit, the velocity can be considered uniform inside the channel, as illustrated in Fig. 1. In the simulations, the thin layer regime is not applicable for the considered values of $k_D w \simeq 5$ and 10. However, the maximum value of the velocity is found to be almost independent from w already when $k_D w > 5$ (see Fig. 1). Therefore, we safely use the value of the velocity

reached on the channel axis in order to compute the EO mobility.

We chose a polymer-coating thickness $\delta = w - h = 5$ nm, that is, about twice the Debye length. The coating is placed on each side of the channel walls, see Fig. 1. The experimentally measured polymer densities, ρ^P , range between 0.1 and 0.18 g/cm³ (see Table 1).

In order to keep the computational model simple, we did not attempt to represent the polymers in full detail, which would take into account their configurational distortion stemming from the EO flow. Rather, the polymers are modeled as fixed scattering centers located at random positions with slabs of distance <5 nm from the wall planes. The scattering centers are immobile, exert a drag force on the moving fluid as specified in Eq. (15) and act as an effective medium. Such a drag can be assimilated to the fluid flow through a porous medium characterized by a friction coefficient γ . In order to obtain a reduction of the EO mobility compatible with the experimental data, we treated it as a fitting parameter with a value $\gamma = 10^{11}$ s⁻¹

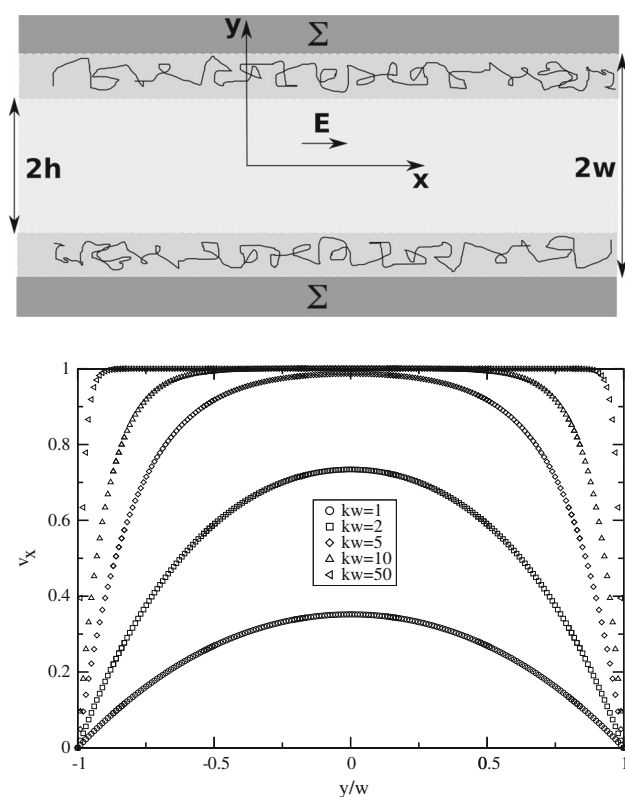


Fig. 1 Upper panel sketch of the capillary with the polymer-free region (light gray), the polymer-coating region (medium gray) and the charged wall (dark gray). In the simulation, the anchored polymers are represented as static scattering centers distributed randomly within the layer region (light gray). The channel width is $2w = 25$ nm, and the polymer-free region is $2h = 7.5$ nm. Lower panel Smoluchowski solution of the velocity profiles in a polymer-free slit channel for different values of y/w and $k_D w$

(see Fig. 1). The number of scattering centers is imposed by calculating the number density of the polymer, being $\rho^P = c\rho^w$, with $0.1 < c < 0.2$. We chose an average value of the polymer density $\rho^P = 0.15$ g/cm³. The friction coefficient γ between the fluid and the scattering centers cannot be derived from first principles, so we took it as a free parameter. As reported in the following, the simulation results exhibit dependence both on the polymer density ρ^P and on the friction coefficient γ .

In a first set of simulations, we considered the case of neutral polymers in order to expose the effect of frictional forces on the EO flow. However, the polymer used in the experiments bears a negative charge. We thus considered a refined version of the coating with each scattering center having a fractional charge. The total amount of polymer charge corresponds to the experimental values, and we considered, in the case of charged polymer, the two extreme experimental conditions corresponding to a total polymer charge of $1e$ and $-1e$. To assign the charge to the scattering centers, we considered the total number of polymers coating the walls and the charge of a single polymer and found that the charge of each scatterer is $q = \pm 10^{-4} e$.

3 Results and interpretation

Figure 2 reports the mobility at varying pH as obtained by experimental measurements and by the simulations, the latter being obtained with the surface charge densities corresponding to a given pH (the procedure used to obtain the correspondence between the surface charge density of

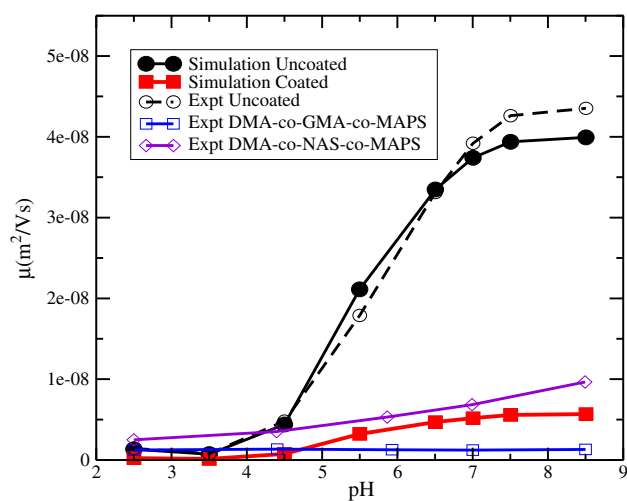


Fig. 2 EO mobility as function of the pH for the uncoated (filled circles) and the coated channels (filled squares) as compared to the experimental curves (open symbols). The values of the surface charge density at different pH are obtained as described in the text

silica, which serves as input parameter for the simulations, and the pH was reported at the end of the previous section). The data in Fig. 2 are obtained for a polymer density of $\rho^P = 0.15 \text{ g/cm}^3$. The experimental curve with higher values of the mobility corresponds to the uncoated case, while the others two curves refer to two different types of polymer coatings.

Figure 3 reports the EO mobility for the same polymer density and friction coefficient used in Fig. 2 but assigning a positive or negative charge to the scattering centers representing the polymer.

Figure 4 displays the EO mobility for different values of the polymer density ρ^P , the friction coefficient γ and for

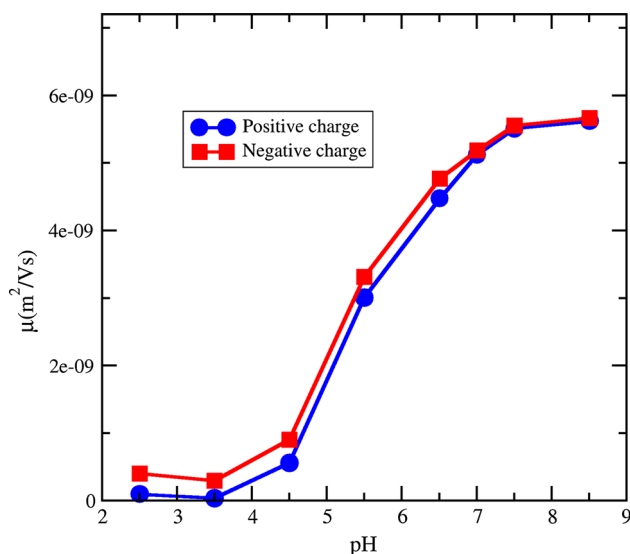
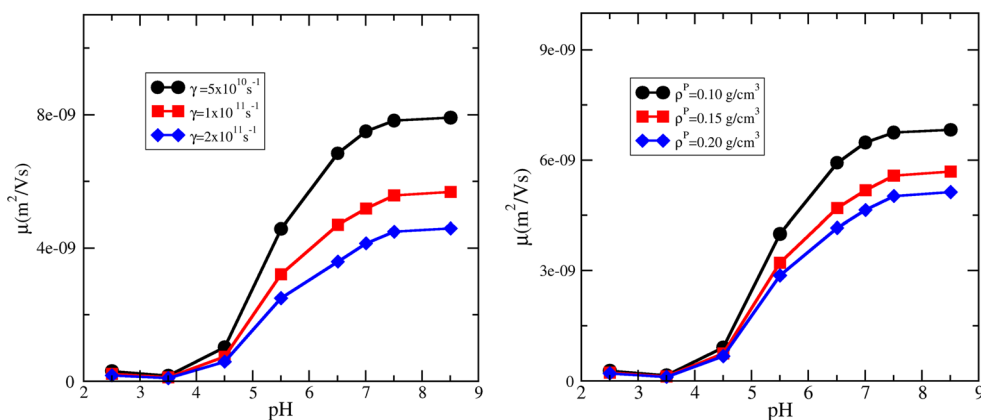


Fig. 3 Simulation results in the case of charged polymer coating with density $\rho^P = 0.15 \text{ g/cm}^3$, thickness 5 nm and $\gamma = 10^{11} \text{ s}^{-1}$. The coating polymers with positive charge produce a decrease of the mobility with respect to the neutral polymers, while negative charge an increase of the mobility. The case of neutral polymers is not reported in the plot, but lies in between the two charged cases

Fig. 4 Simulation results for the EO mobility at given density $\rho^P = 0.15 \text{ g/cm}^3$ and at varying friction (*left*); EO mobility at given friction $\gamma = 10^{11} \text{ s}^{-1}$ and varying polymer density (*right panel*). Data refer to a polymer thickness of 5 nm



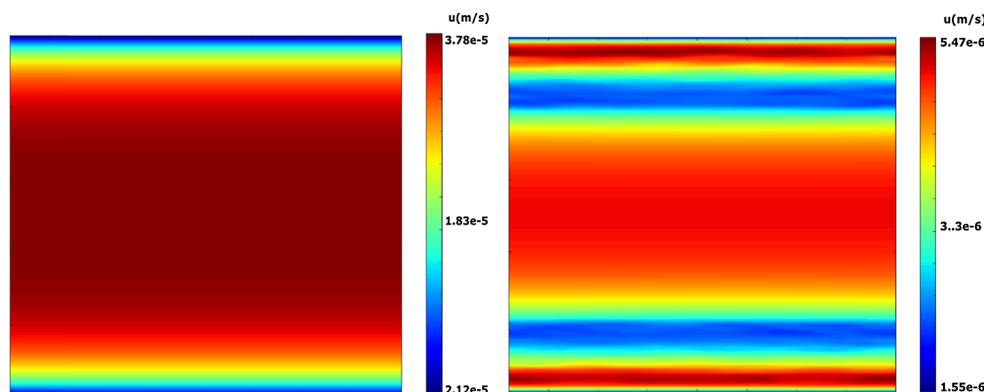
charged coating polymers. It is appreciated that the mobility decreases for increasing polymer-coating densities and friction, and altogether, the curves show a certain dependence on these parameters.

Analogously to the simulation setup, a theoretical understanding of the observed EO flow reduction requires to mimic the polymer-rich region at an acceptable level. To this aim, we considered an effective model for the polymers anchored on the walls. We preliminarily observe that the presence of the polymers modeled as a neutral medium, while not affecting the charge distribution inside and outside the polymer layer, can substantially reduce the velocity field of the ions in the coated region as compared to the polymer-free region.

The fact that the distribution of the mobile ions along the direction transverse to the flow is taken to be the same as in the absence of the polymer arises from the observation that the polymer charge is a small fraction of the surface charge. In addition, it is reasonable to neglect excluded volume forces arising from the polymer, an assumption that holds if the polymer number density is mostly uniform along the transversal direction and if the dielectric permittivity of the polymer-rich region is similar to that in the polymer-free one. Therefore, in our theoretical treatment, we neglect the charge on the polymers and consider the coating region as an effective and homogeneous Darcy medium, thereby expecting a finite slip length at the polymeric interface. Implicitly, we also consider such interface to have a smooth profile. Typical velocity contours for the uncoated and coated channels are shown in Fig. 5, showing the rather nontrivial behavior inside and outside the coating.

At the walls, the electric potential, $\phi(\pm w) = \zeta$, is governed by a diffusive equilibrium, while the velocity of the electrolytic solution obeys a no-slip condition on the wall, $v_x(\pm h) = 0$. The electrostatic potential is governed by the Poisson–Boltzmann equation

Fig. 5 Contour maps of the velocity profile in the uncoated (left) and coated (right) slit channel. The right panel refers to a coating thickness of 5 nm and density $\rho^P = 0.15 \text{ g/cm}^3$ and $\gamma = 10^{11} \text{ s}^{-1}$



$$\epsilon \frac{d^2 \phi(y)}{dy^2} = -n_B e \sinh(e\beta \phi(y)) \tag{6}$$

and, by linearizing Eq. (6) (small field approximation), $\frac{d^2 \phi(y)}{dy^2} = k_D^2 \phi(y)$ the solution is $\phi(y) = \zeta \frac{\cosh(k_D y)}{\cosh(k_D h)}$. The velocity field is governed by a Stokes equation only in the polymer-free region,

$$\eta \frac{d^2 v(y)}{dy^2} = \epsilon E_x \frac{d^2 \phi(y)}{dy^2}, \tag{7}$$

while in the polymeric region, the fluid experiences an additional frictional force and the Stokes–Smoluchowski equation modifies as

$$\eta \frac{d^2 v(y)}{dy^2} - \gamma \rho^w v(y) = \epsilon E_x \frac{d^2 \phi(y)}{dy^2}. \tag{8}$$

In Eq. (8), the effect of the polymer friction, represented by the second term in the left-hand side, is modeled via a phenomenological Brinkman contribution (Wijmans and Smit 2002). By combining with the electrostatic potential profile, and defining $\alpha = \sqrt{\gamma \rho^w / \eta}$, the explicit solution in the polymeric region $h < |y| < w$ is

$$v_x(y) = \frac{\epsilon E_x}{\eta} \zeta \frac{k_D^2}{k_D^2 - \alpha^2} \left[\frac{\cosh(k_D y)}{\cosh(k_D w)} - \frac{\cosh(\alpha y)}{\cosh(\alpha w)} \right] \tag{9}$$

and in the polymer-free region, $|y| < h$,

$$v_x(y) = \frac{\epsilon E_x}{\eta} \zeta \frac{\cosh(k_D h)}{\cosh(k_D w)} \left[\frac{\cosh(k_D y)}{\cosh(k_D h)} - 1 \right] + v_{sl}. \tag{10}$$

The term

$$v_{sl} = \frac{\epsilon E_x}{\eta} \zeta \frac{k_D^2}{k_D^2 - \alpha^2} \left[\frac{\cosh(k_D h)}{\cosh(k_D w)} - \frac{\cosh(\alpha h)}{\cosh(\alpha w)} \right] \tag{11}$$

can be interpreted as a slip velocity at the polymeric interface, and it guarantees that the total solution is continuous in $y = \pm h$. At small value of α , the maximum fluid velocity is located at the center of the channel, while for large values, two maxima appear in the polymeric region.

To appreciate the quality of the analytical model, we compare the simulated and analytical velocity profiles in Fig. 6. In the polymer-free region, the agreement between the two curves is excellent in all considered cases, while some discrepancy is present in the polymer-rich region. Using a coating thickness of 5 nm, Fig. 6 (left panels) reports the data for two values of the polymer density, $\rho^P = 0.15$ and 0.1 g/cm^3 , and with the length α^{-1} corresponding to 1 nm. A better agreement is obtained by increasing the polymer density, while lowering the coating thickness to 2.5 nm, a value comparable to the Debye length, the quality of the agreement is also stronger as compared to the case of larger thickness (Fig. 6, upper right panel).

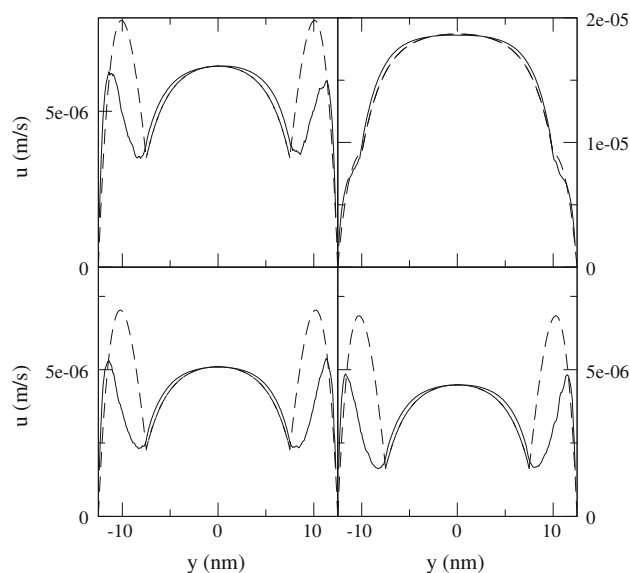


Fig. 6 Velocity profiles of the mixture obtained for polymer density and thickness of the coating equal to 0.1 g/cm^3 , 5 nm (upper left), 0.15 g/cm^3 , 2.5 nm (upper right), 0.15 g/cm^3 , 5 nm (lower left), 0.2 g/cm^3 , 5 nm (lower right) and $\gamma = 10^{11} \text{ s}^{-1}$. Solid lines correspond to the simulations and the dashed lines to the theoretical predictions

4 Conclusions

Polymer coatings are often employed in capillary electrophoresis in order to control the EO flow and to minimize wall–analyte interactions. A substantial reduction of EO flow is observed when the thickness of the coating layer is comparable to the Debye length.

The EO flow originates from the surplus of counter-ions within the double layer, that is, in the region where the attraction toward the walls is maximal and partially compensated by diffusional forces. EO flow is generated by a small portion of counter-ions, as compared to the globally available charges, that is capable of dragging along the same direction the whole electrolytic solution, the so-called conveyor belt mechanism.

In the presence of the polymer coating, experiments and simulation have observed a substantial quench of the EO flow. It is plausible that the momentum imparted on the counter-ions is effectively transferred to the anchored polymers. Such mechanism could not be the only one in place. In fact, a sufficient momentum imparted on the counter-ions could create sufficient strain in the fluid and thus maintain sufficient EO flow even away from the polymer-rich region. In the latter case, more sophisticated effects could arise due to a substantial modification of the Debye layer, that is, by a distortion of the double layer due to shearing forces.

In this paper, we analyzed the problem from three different points of view. In fact, while in the experiments, the polymers are effectively anchored to the wall and can distort their conformation in order to accommodate the flow, our simulation model considers the coating layer as a system of static and randomly distributed scatterers whose role is solely to remove a fraction of momentum via frictional forces. The theoretical model considers the coating as an effective Darcy medium, homogeneous along the flow direction. In essence, the simulation model represents the polymer-rich region alike a porous medium, whereas the theoretical model further simplifies it to a Darcy medium.

The simulation data provided evidence that the frictional forces alone are sufficient to suppress the EO flow and the velocity profiles show negligible residual velocities in the polymer-rich region. Implicitly, this means that the transversal charge distribution still obeys a Poisson–Boltzmann type of equilibrium. Thus, the usual Smoluchowski picture of decoupling the equilibrium solution along the orthogonal direction from the off-equilibrium solution along the flow direction still holds. Under such circumstances, the analytical flow profile can be derived and shows good agreement with the velocity profiles obtained in simulation. The largest discrepancy is in the polymer-rich region, which is still acceptable given the simple theoretical model employed. Notwithstanding the differences in the coating, a fact that

could generate relevant qualitative differences in the mass transport, the flow rates are insensitive to such details. As the mesoscopic simulations reveals, the quenching of the EO mobility is correctly captured by our model.

The situation remains basically unchanged when the scatterers are taken as slightly charged, in order to reproduce as closely as possible the polymer coatings used in experiments. Such distributed charges, however, are weak competitors against the surface charges and only distort marginally the double layer. Therefore, the reduction of EO flow is still strong and the amount of reduction is quantitatively reproduced.

In the future, it will be interesting to analyze the regime of small polymer concentration in which both the uniform distributions of scatterers are not expected to hold any longer. In fact, at small concentrations, polymers organize in mushroom configurations and such inhomogeneity can produce unexpected behavior on the ionic currents and the EO flow. Another interesting regime is when the coating thickness is much smaller than the Debye length, that is, when the ionic currents are still substantial at the polymer-rich/polymer-free interface. It is possible that interesting slip length effects take place under such conditions and require an adequate theoretical treatment.

Acknowledgments This work was partially supported by the Italian Ministry of University and Research through the “Futuro in Ricerca” Project RBFR12001G—NEMATIC.

Appendix: Kinetic treatment of electroosmotic flows

The equations governing the motion of the electrolytic solution are solved at the level of kinetic theory for a ternary mixture of species, one for the neutral solvent and two for the counter and co-ions, respectively. We name the species number densities, $n^z = n^0, n^+, n^-$, having equal unit masses and valence $z^z = 0, 1, -1$ for a 1:1 electrolytic solution (Melchionna and Marconi 2011, 2012).

The scatterers are located at random positions $\{R\}$ within the coating layer and may or may not be neutral. In the latter case, each scatterer bears a constant charge eq. The electric potential is thus given by the solution of the Poisson equation

$$\nabla^2 \phi = -\frac{e}{\epsilon} \left(n^+ - n^- + q \sum_R \delta(r - R) \right) \quad (12)$$

Subjected to the boundary condition

$$(\nabla \phi)_\perp = -\frac{\Sigma}{\epsilon} \quad (13)$$

where the subscript \perp indicates the component of the electric field normal and outward from the walls and

having local charge density Σ . The presence of a voltage difference between the inlet and outlet of the channel is accounted for by a homogeneous electric field acting on the charged species.

The mixture is represented in terms of a set of three distribution function $f^\alpha(x, v, t)$, being the probability of having a particle of species α at position x , with velocity v and at time t . The evolution of each species obeys the equation

$$\partial_t f^\alpha + \nabla \cdot v f^\alpha = \omega \left(f_{\text{eq}}^\alpha - f^\alpha \right) + \frac{e z^\alpha}{m} \nabla \phi \cdot \frac{\partial}{\partial v} f^\alpha - \frac{F^{\text{scatt}}}{m} \cdot \frac{\partial}{\partial v} f^\alpha \equiv Q^\alpha \quad (14)$$

where $f_{\text{eq}}^\alpha = \left[\frac{m}{2\pi k_B T} \right]^{3/2} n^\alpha e^{-\frac{m(v-u)^2}{2k_B T}}$ is the Maxwell–Boltzmann local equilibrium, $u = \sum_\alpha n^\alpha u^\alpha / \sum_\alpha n^\alpha$ is the barycentric fluid velocity, and u^α is the specie velocity. The quantity ω controls the rate of relaxation toward local equilibrium and is related to the kinematic viscosity. Finally, F^{scatt} represents the effect of the frictional force arising from the scatterers, modeled as

$$\frac{F^{\text{scatt}}}{m} = -\gamma \sum_R u^\alpha \delta(r - R) \quad (15)$$

where γ is the friction coefficient.

The electrokinetic equations are solved numerically in the framework of the LB method. In essence, the distributions f^α are discretized in space over a Cartesian mesh and expanded in velocity space over a Hermite basis set. By expressing the Hermite expanded version of the distributions f^α as f_p^α and analogously for RHS of Eq. (14) Q^α as Q_p^α , the distributions are evolved in time according to the scheme

$$f_p^\alpha(r + c_p, t + 1) - f_p^\alpha(r, t) = Q_p^\alpha(r, t) \quad (16)$$

Here, c_p represents a set of discrete speed that connects a mesh point to its neighbor mesh points. Starting from the f_p^α , the fluid density and velocity can be computed as

$$n^\alpha = \sum_p f_p^\alpha \quad (17)$$

and

$$n^\alpha u^\alpha = \sum_p c_p f_p^\alpha \quad (18)$$

For the numerical solution, we employed the so-called D3Q19 discretization scheme, consisting of 19 discrete speeds and a full three-dimensional solution of the equations of motion. Specific information on the numerical method can be found in Melchionna and Marconi (2011, 2012).

References

- Benzi R, Succi S, Vergassola M (1992) The Lattice Boltzmann equation: theory and applications. *Phys Rep* 222(3):145–197
- Bruus H (2008) Theoretical microfluidics. Oxford University Press, Oxford
- Cao Q, Zuo C, Li L, Ma Y, Li N (2010) Electroosmotic flow in a nanofluidic channel coated with polymers. *Microfluid Nanofluid* 9:1051–1062
- Chiari M, Cretich M, Damin F, Ceriotti L, Consonni R (2000) New adsorbed coatings for capillary electrophoresis. *Electrophoresis* 21(5):909–916
- Doherty EAS, Berglund KD, Buchholz BA, Kourkine IV, Przybycien TM, Tilton RD, Barron AE (2002) Critical factors for high-performance physically adsorbed (dynamic) polymeric wall coatings for capillary electrophoresis of DNA. *Electrophoresis* 23:2766–2776
- Grass GW, Holm K, Slater GW (2009) Optimizing end-labeled free-solution electrophoresis by increasing the hydrodynamic friction of the drag tag. *Macromolecules* 42(14):5352–5359
- Grier DG, Behrens SH (2001) The charge of glass and silica surfaces. *J Chem Phys* 115(14):6716
- Harden JL, Long D, Ajdari A (2001) Influence of end-grafted polyelectrolytes on electro-osmosis along charged surfaces. *Langmuir* 17:705–715
- Hickey OA, Harden JL, Slater GW (2009a) Molecular dynamics simulations of optimal dynamic uncharged polymer coatings for quenching electro-osmotic flow. *Phys Rev Lett* 102(10):108304
- Hickey OA, Harden JL, Slater GW (2009b) Molecular dynamics simulations of optimal dynamic uncharged polymer coatings for quenching electro-osmotic flow. *Phys Rev Lett* 102:108304
- Hickey OA, Holm C, Harden JL, Slater GW (2011) Influence of charged polymer coatings on electro-osmotic flow: molecular dynamics simulations. *Macromolecules* 44:9455–9463
- Horvath J, Dolník V (2001) Polymer wall coatings for capillary electrophoresis. *Electrophoresis* 22(4):644–655
- Masliyah JH, Bhattacharjee S (2006) Electrokinetic and colloid transport phenomena. Wiley, London
- Melchionna S, Marconi UBM (2011) Electro-osmotic flows under nanoconfinement: a self-consistent approach. *Eur Phys Lett* 95:44002
- Melchionna S, Marconi UBM (2012) Charge transport in nanochannels: a molecular theory. *Langmuir* 28(38):13727–13740
- Quiao R, He P (2007) Modulation of electroosmotic flow by neutral polymers. *Langmuir* 23:5810
- Slater GW et al (2009) Modeling the separation of macromolecules: a review of current computer simulation methods. *Electrophoresis* 30(5):792–818
- Sola L, Chiari M (2012) Modulation of electroosmotic flow in capillary electrophoresis using functional polymer coatings. *J Chromatogr A* 1270:324–329
- Tessier F, Slater GW (2005) Control and quenching of electroosmotic flow with end-grafted polymer chains. *Macromolecules* 38(16):6752–6754
- Tessier F, Slater GW (2006) Modulation of electroosmotic flow strength with end-grafted polymer chains. *Macromolecules* 39(3):1250–1260
- Wijmans CM, Smit B (2002) Simulating tethered polymer layers in shear flow with the dissipative particle dynamics technique. *Macromolecules* 35:7138–7148
- Williams BA, Vigh G (1996) Fast, accurate mobility determination method for capillary electrophoresis. *Anal Chem* 68(7):1174–1180
- Znalezionia J, Petr J, Knob R, Maier V, Ševčík J (1999) Dynamic coating agents in CE. *Chromatographia* 67(1):5–12